


# Very Persistent Random Walkers Reveal Transitions in Landscape Topology

Jaron Kent-Dobias<sup>1</sup>\*

*ICTP South American Institute for Fundamental Research, São Paulo, Brazil  
and Instituto de Física Teórica, Universidade Estadual Paulista “Júlio de Mesquita Filho,” São Paulo, Brazil*

 (Received 25 May 2025; revised 1 January 2026; accepted 2 March 2026; published 18 March 2026)

We study the typical behavior of random walkers on the microcanonical configuration space of mean-field disordered systems. Passive walks have an ergodicity-breaking transition at precisely the energy density associated with the dynamical glass transition, but persistent walks remain ergodic at lower energies. In models where the energy landscape is thoroughly understood, we show that, in the limit of infinite persistence time, the ergodicity-breaking transition coincides with a transition in the topology of microcanonical configuration space. We conjecture that this correspondence generalizes to other models, and use it to determine the topological transition energy in situations where the landscape properties are ambiguous.

DOI: 10.1103/jvvpw-csk7

**Introduction**—The notion of an energy landscape and ideas about its geometry and topology influence our understanding of diverse phenomena, including glasses [1], spin glasses [2], proteins [3], evolution [4], ecosystems [5], and machine learning [6,7]. As landscapes in high-dimensional space, one cannot understand their geometry and topology by making a topographical map. Instead, one must make sense of the low-dimensional shadows they cast, either through projection along a few important axes [8–11] or by studying kinds of summary statistics. The most important summary statistic for understanding complex landscapes is the entropy of their minima and saddle points, often called complexity [12–15].

The most commonly invoked feature of the complexity is the level at which the population of minima begins to outnumber the population of saddle points, known as the threshold energy  $E_{th}$ . This transition is heuristically thought as a point of landscape flatness (a geometric property) [16] and landscape percolation (a topological property), both important for explaining why the threshold should attract slow asymptotic dynamics [17]. However, recent work has called into question the threshold’s monopoly on flatness [18–22] and its significance to dynamics [19,23,24] and landscape topology [25].

Here, we focus on a question of topology: at what level in the landscape do typical points in configuration space transition from being smoothly connected to being isolated? To answer this question, we look at the dynamics of random walkers confined to a specific energy level. If a random walk from a typical initial condition can travel arbitrarily far from its starting point, i.e., is ergodic, we conclude that the level set of the energy, or the microcanonical configuration space at that energy, is typically connected.

Unfortunately, the converse is not true: random walks are often not ergodic on a connected configuration space. We will see that for passive walkers, there is a direct correspondence between microcanonical and canonical dynamics, with the ergodicity-breaking transition for the random walk occurring at precisely the energy density of the dynamical glass transition. The transition is driven by entropic barriers, not topology: there is nothing remarkable about the energy landscape at this energy density.

Fortunately, there are other kinds of random walkers. Persistent or active random walks, where the walker tends to step in the same direction over a persistence time  $\tau_0$ , appear often in biological and biology-inspired settings where the walker expends energy to drive itself forward until its direction is changed either by random noise or by its own volition [26]. Active systems are known to be good at crossing barriers, entropic or otherwise [27–30]. Activity is also known to drive the glass transition to lower temperatures [31,32]. In what follows, we see that persistent walkers remain ergodic at lower energies than passive ones. Moreover, we argue that, in the limit of infinite persistence time, the ergodicity-breaking transition coincides with the transition in the landscape topology from typically connected to typically disconnected. A cartoon of this scenario is shown in Fig. 1.

A similar result was recently found in the random Lorentz gas, a simplified model of the structural glass transition involving a tracer moving freely between fixed spherical obstacles of some density. When the tracer is passive, there is a separation between the densities of the dynamical glass transition and the percolation transition [33–35]. On the other hand, an active tracer sees its ergodicity-breaking transition pushed toward the percolation transition with increasing activity [36]. Our results suggest this is the manifestation of a generic phenomenon.

\*Contact author: jaron@ictp-saifr.org

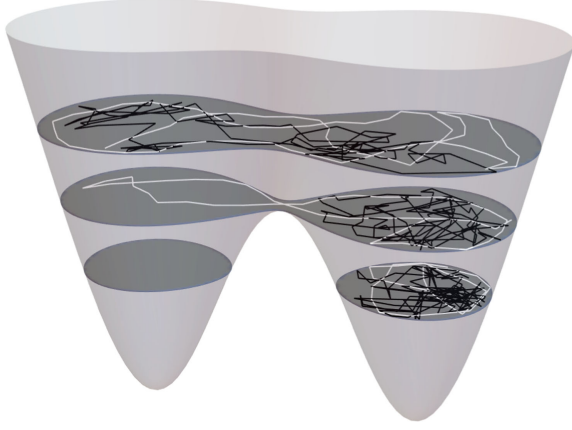


FIG. 1. The behavior of a passive (black) and persistent (white) random walker on level sets of a cartoon landscape. The persistent walker remains ergodic at lower energies than the passive one. Increasing persistence pushes the ergodic transition of the walk toward a topological transition of the landscape associated with the typical connectivity of configurations.

Infinitely persistent activity has also been used to probe properties of the energy landscape in glasses, both in mean-field and in finite dimensions [37–40].

*The model*—We consider the position  $\mathbf{x} \in \mathbb{R}^N$  of a random walker driven by Gaussian noise  $\xi$  with zero mean and with variance

$$\langle \xi_i(t) \xi_j(s) \rangle = \delta_{ij} \Gamma(t-s) \quad (1)$$

for a kernel  $\Gamma$  depending only on the time difference. In this Letter we typically use an exponentially decaying kernel,

$$\Gamma(\tau) = \frac{1}{\tau_0} e^{-|\tau|/\tau_0}, \quad (2)$$

with characteristic persistence time  $\tau_0$ . In the limit of zero  $\tau_0$ ,  $\Gamma$  approaches a Dirac  $\delta$  function and the noise is Markovian, and we say the walker is passive. The walker moves freely besides two constraints: it is confined to the sphere  $\|\mathbf{x}\|^2 = N$  due to the model, and it is confined to the constant-energy level set  $H(\mathbf{x}) = EN$ . Such a random walk can be described by the Langevin equation

$$\frac{\partial \mathbf{x}(t)}{\partial t} = \xi(t) - \mu(t) \mathbf{x}(t) - \beta(t) \nabla H(\mathbf{x}(t)), \quad (3)$$

where  $\mu$  and  $\beta$  are time-dependent parameters that adjust the magnitude of forces perpendicular to the constraint manifolds in order to prevent the walker from leaving them. The dynamics of our walker are equivalent to that of an Ornstein–Uhlenbeck particle traversing the configuration space [41]. Ignoring the spherical constraint, this framework is general: a system of  $P$  active Brownian particles in  $d$  dimensions is captured by configurations  $\mathbf{x}$  in  $N = Pd$  dimensions concatenating the positions of each particle.

We take our model to be a spherical spin glass, a family of mean-field models of glassy behavior whose properties are closely related to the random first order and mode-coupling theories of the glass transition [42–45]. In equilibrium, they undergo a dynamical transition that breaks ergodicity without passing an equilibrium phase transition. The Hamiltonian  $H$  is a random polynomial of the components of  $\mathbf{x}$  with independent centered Gaussian coefficients, or

$$H(\mathbf{x}) = \sum_{p=0}^{\infty} \frac{1}{p!} \sqrt{\frac{f^{(p)}(0)}{N^{p-1}}} \sum_{i_1, \dots, i_p} J_{i_1, \dots, i_p}^{(p)} x_{i_1} \cdots x_{i_p}, \quad (4)$$

where the  $J$  are centered Gaussian with  $\overline{J^2} = 1$  [46,47]. The composition of the random polynomial is compactly encoded in a function  $f$  whose series coefficient at order  $p$  gives the relative strength of the degree- $p$  contribution to  $H$ . The function  $f$  also gives the covariance between  $H$  evaluated at two different points in space, with

$$\overline{H(\mathbf{x})H(\mathbf{x}')} = Nf\left(\frac{\mathbf{x} \cdot \mathbf{x}'}{N}\right). \quad (5)$$

The pure  $p$ -spin models have  $H$  a homogeneous polynomial of degree  $p$  and  $f(q) = \frac{1}{2}q^p$ , while all other models are referred to as mixed. In this Letter, we refer to equally appointed mixed models with  $f(q) = \frac{1}{4}(q^p + q^s)$  as  $p + s$ -spin.

The complexity of these models has been extensively studied [13,14,18,48–52], and so long as there is not replica symmetry breaking among stationary points [20,53] the threshold energy below which minima outnumber saddle points is

$$E_{\text{th}} = -\frac{f'(1)^2 + f(1)(f''(1) - f'(1))}{f'(1)\sqrt{f''(1)}}. \quad (6)$$

In the pure spherical spin glasses the threshold energy is unambiguously significant in the landscape geometry and topology because it is a sharp boundary between populations of minima and saddle points, and this is reflected in its importance to out-of-equilibrium dynamics [16,17]. In mixed models the boundary is not sharp, with exponentially many minima found above the threshold and exponentially many saddle points found below it. In this setting, the topological and geometric significance of the threshold is not obvious. Sketches of the topology of the energy level sets of pure and mixed models are shown in Fig. 2. We find that the ergodicity-breaking transition of infinitely persistent random walkers coincides with the threshold in certain mixed models, conditionally validating its topological significance.

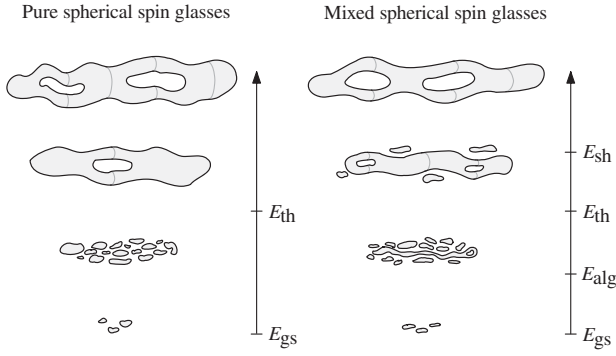


FIG. 2. Schematic depiction of the energy level set topology of spherical spin glasses as energy density is varied. The threshold  $E_{\text{th}}$  is defined by the energy at which minima begin to outnumber saddle points. In pure models the level set is connected above  $E_{\text{th}}$ , while no connected component exists below  $E_{\text{th}}$ . In mixed models the breaking up of the level set occurs over a range of energies.  $E_{\text{alg}}$  is the lowest energy at which a large connected component of the level set exists [54], while  $E_{\text{sh}}$  marks where the Euler characteristic of the level set changes sign [25]. In pure models,  $E_{\text{th}} = E_{\text{alg}} = E_{\text{sh}}$ . An aim of this Letter is to determine the lowest energy at which typical parts of the level set belong to a large connected component.

*The dynamical equations*—We seek asymptotic solutions to the correlation and response functions resulting from the Langevin equation (3) averaged over noise  $\xi$  and disorder  $J$  in the limit of large  $N$ . If a deterministic source  $\mathbf{h}(t)$  is added to the equation of motion, these dynamic order parameters are

$$C(t, s) = \frac{1}{N} \overline{\langle \mathbf{x}(t) \cdot \mathbf{x}(s) \rangle}, \quad R(t, s) = \frac{1}{N} \sum_{i=1}^N \left. \overline{\left\langle \frac{\delta x_i(t)}{\delta h_i(s)} \right\rangle} \right|_{\mathbf{h}=0}, \quad (7)$$

respectively. We seek time-translation invariant solutions where the order parameters take the form  $C(t + \tau, t) = C(\tau)$ ,  $R(t + \tau, t) = R(\tau)$ ,  $\mu(t) = \mu$ , and  $\beta(t) = \beta$  independent of  $t$ . The random walk will be judged ergodic if the correlation function  $C$  decays to zero at large time difference  $\tau$ . Employing standard methods detailed in the End Matter [55], the typical behavior of the correlation and response functions averaged over realizations of the noise and of the disorder obey integrodifferential equations of the form

$$\begin{aligned} \left( \frac{\partial}{\partial \tau} + \mu \right) C(\tau) &= 2 \int d\sigma \Gamma(\tau - \sigma) R(-\sigma) \\ &+ \beta^2 \int d\sigma R(\tau - \sigma) f''(C(\tau - \sigma)) C(\sigma) \\ &+ \beta^2 \int d\sigma f'(C(\tau - \sigma)) R(-\sigma), \end{aligned} \quad (8)$$

$$\begin{aligned} \left( \frac{\partial}{\partial \tau} + \mu \right) R(\tau) &= \delta(\tau) + \beta^2 \int d\sigma R(\tau - \sigma) f''(C(\tau - \sigma)) \\ &\times R(\sigma), \end{aligned} \quad (9)$$

along with equations

$$E = -\beta \int d\tau f'(C(\tau)) R(\tau), \quad 1 = C(0), \quad (10)$$

fixing the values of  $\beta$  and  $\mu$ . Together, these equations imply a generalized fluctuation-dissipation relation of the form

$$R(\tau) = -\Theta(\tau) \int d\sigma \Gamma^{-1}(\tau - \sigma) C'(\sigma), \quad (11)$$

where  $\Theta$  is the Heaviside function and  $\Gamma^{-1}$  is the inverse of  $\Gamma$  under convolution. For the noise kernel (2) with persistence time  $\tau_0$ ,  $\Gamma^{-1}(\tau) = \delta(\tau) - \tau_0^2 \delta''(\tau)$ , which gives  $R(\tau) = -\Theta(\tau) [C'(\tau) - \tau_0^2 C'''(\tau)]$ . This latter relation resembles ones previously derived for active Ornstein–Uhlenbeck particles [41,56]. The generic relation (11) should hold in general for processes driven by noise (1) under deterministic forces derived from a potential.

*Exact behavior*—When  $\tau_0 = 0$  and the random walk is passive, these dynamical equations correspond to those for the canonical equilibrium dynamics of the model at the temperature  $T$  whose average energy density is  $E$ , but with time rescaled by a constant factor. This implies the equivalence of the microcanonical and canonical dynamics. Therefore, the ergodicity-breaking transition of the walker occurs at the energy density corresponding to the dynamical glass transition temperature  $T_d$ , where

$$T_d = \sqrt{\frac{1 - q_d}{q_d}} f'(q_d), \quad 1 - q_d = \frac{f'(q_d)}{q_d f''(q_d)}, \quad (12)$$

which in these models implies  $E_d = -f(1)/T_d$ .

The ergodicity-breaking transition for  $\tau_0 = 0$  does not correspond to any qualitative change in the microcanonical configuration space, but rather is a result of entropic barriers. We can clearly show this in the situation where the equations are exactly solvable, for the pure 2-spin model with  $f(q) = \frac{1}{2} q^2$ . Here, the energy landscape is not complex: it has two symmetrically related minima with energy density  $E = -1$ , and its microcanonical configuration space spans all overlaps and has the same topology for all energy densities  $-1 < E < 0$ . Nevertheless, the dynamical glass transition energy with  $\tau_0 = 0$  is  $E_d = -\frac{1}{2}$ , an unremarkable level in the landscape.

A persistent walker maintains ergodicity to much lower energy densities. In the solvable 2-spin model, the energy density of the ergodicity-breaking transition is given as a function of  $\tau_0$  by

$$E_{\text{erg}}(\tau_0) = -1 + \frac{1}{\sqrt{3\tau_0}} \sinh \left[ \frac{1}{3} \sinh^{-1} \left( \frac{3}{2} \sqrt{3\tau_0} \right) \right], \quad (13)$$

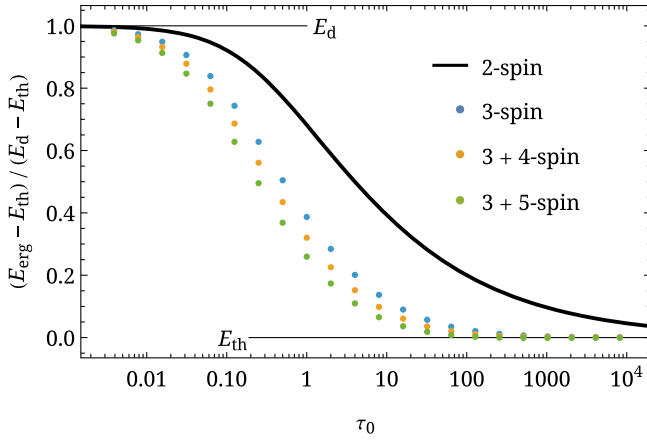


FIG. 3. The ergodicity-breaking transition energy as a function of persistence time  $\tau_0$  of an active random walker on the microcanonical configuration space of several spherical spin glasses. The solid black line is the explicit solution (13) for the pure 2-spin model, while the points show numeric estimates for several other models.

which interpolates between  $E_{\text{erg}}(0) = E_d = -\frac{1}{2}$  and  $E_{\text{erg}}(\infty) = E_{\text{th}} = -1$  and is plotted in Fig. 3. Therefore, in the pure 2-spin model an infinitely persistent walker preserves ergodicity down to the energy density at which a topological change in the landscape makes ergodicity impossible. In what follows, we argue that this property continues to hold in other models.

*Numeric solutions*—These equations lack an important feature usually exploited to numerically solve them: (8) at a given time depends on the value of  $C$  for all times previous, including all negative times. This scenario arises whenever detailed balance is violated [31,57,58]. Hence one cannot solve the equations by beginning at  $\tau = 0$  and stepping forward as is often done. In order to produce numeric solutions, we solve the equations by iteration starting from the exact solution for  $C$  and  $R$  when  $E = 0$ . Details of this procedure can be found in the End Matter.

We estimate the energy of the ergodicity-breaking transition for a given persistence time  $\tau_0$  by numerically solving the dynamical equations for successively smaller  $E$  until the Fourier transform of the correlation function  $C$  develops a singularity at  $\hat{C}(\omega = 0)$ , which signals the presence of a plateau in the correlation function at nonzero overlap  $q$  with the initial condition. Estimates of these transition energies assuming the divergence of  $\hat{C}(0)$  is a power law like in equilibrium [59–61] are plotted in Fig. 3 for pure and mixed models. In both, increasing  $\tau_0$  smoothly interpolates between the dynamical glass transition energy and the threshold energy where minima begin to outnumber saddle points.

As the persistence of the walker increases, not only the energy of the transition changes, but also the overlap  $q = C(\infty)$  associated with the loss of ergodicity grows toward  $q = 1$ . This is reflected in Fig. 4, which plots  $C$  near

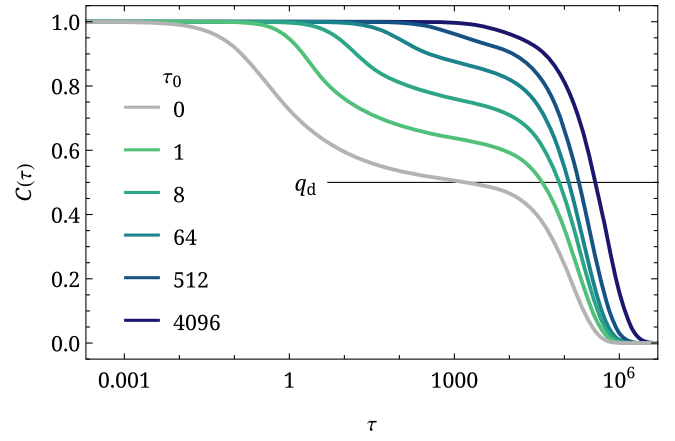


FIG. 4. The correlation function for the pure 3-spin spherical spin glass at several values of the persistence time  $\tau_0$ . The plateau overlap  $q_d$  of the equilibrium dynamical transition of  $\tau_0 = 0$  is marked. As  $\tau_0$  increases, the plateau of the ergodicity-breaking transition moves to higher overlaps. The energies associated in order of increasing  $\tau_0$  are  $-0.8157$ ,  $-1.0230$ ,  $-1.1076$ ,  $-1.1421$ ,  $-1.1517$ , and  $-1.1538$ , whereas  $E_d \simeq -0.8165$ , and  $E_{\text{th}} \simeq -1.1547$ .

the transition energy for a variety of persistence times  $\tau_0$ . Each correlation function shows a characteristic bump in the decay, and the increasing value of  $C$  at the bump indicates the growing  $q$ . In the limit of infinite persistence, the asymptotic overlap at the transition appears to grow to  $q = 1$ . The ratio  $\mu/\beta$  at the transition approaches  $\sqrt{4f''(1)}$

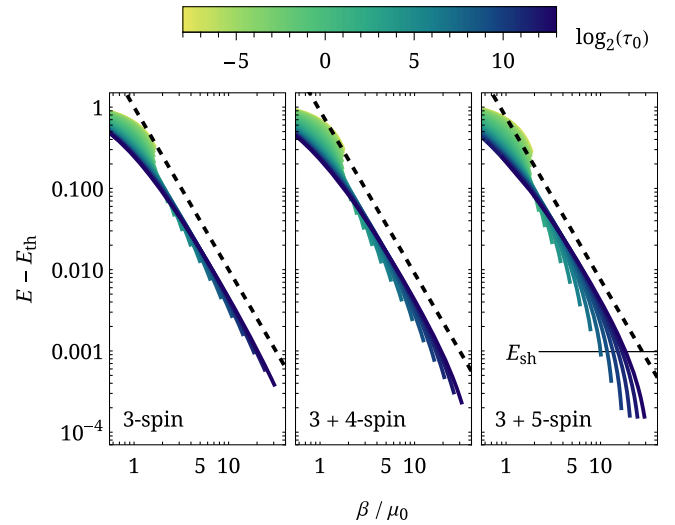


FIG. 5. Energy difference above the threshold energy as a function of  $\beta/\mu_0$ , where  $\mu_0$  is the value of  $\mu$  associated with a free persistent random walk given by (C2). Each line shows the behavior at fixed persistence time for  $\tau_0 = 2^{-8}, 2^{-7}, \dots, 2^{13}$ , with larger  $\tau_0$  corresponding to lower endpoints. The dashed black line is an inverse-square power law  $\beta^{-2}$ . In the 3 + 5-spin model, a horizontal line shows the location of  $E_{\text{sh}}$  defined in Ref. [25] where another aspect of the landscape topology undergoes a transition.

at infinite persistence time, something perhaps related to marginality.

We cannot precisely measure the asymptotic energy by fitting  $\hat{C}(0)$  as a function of  $E$  because the power law associated with its divergence is not known in general. However, in the exact solution for the pure 2-spin model at infinite persistence time, the energy is related to the parameter  $\beta$  by  $E = E_{\text{erg}} + \frac{1}{2}\beta^{-2} + O(\beta^{-4})$  for  $\beta \rightarrow \infty$ . This scaling behavior appears to also hold in other models, which allows us to precisely identify the ergodic transition at infinite persistence time. This increasingly power-law approach of the energy to the threshold with increasing  $\tau_0$  is shown in Fig. 5 for the three nontrivial models studied here. Other prospective transition energies, like that associated with a topological invariant introduced in Ref. [25], are clearly ruled out. In all three cases, our data suggest that the threshold energy  $E_{\text{th}}$  is the ergodic transition energy in the infinitely persistent limit.

In the pure spherical models the dynamic, geometric, and topological significance of the threshold energy is not ambiguous. The fact that at infinite persistence time the ergodic transition reaches this topologically significant point leads us to conjecture that this behavior is generic: that the energy level of the ergodicity-breaking transition for an infinitely persistent walker is topologically significant, in the sense that under it typical points in configuration space do not belong to the same connected component. Based on this conjecture and the numeric data discussed above, we therefore conclude that this topological transition takes place at  $E_{\text{th}}$  also in the mixed spherical models examined here.

*Conclusions*—We have developed a dynamical mean-field theory of persistent random walks on the microcanonical configuration space of models with complex landscapes. Based on an exact solution and on approximate numeric solutions for the well-understood pure  $p$ -spin spherical models, we conjecture that an infinitely persistent walker remains ergodic until a topological transition in the configuration space is passed. By further examining numeric solutions on the less-understood mixed spherical models, we argue that the ergodicity-breaking transition at infinite persistence time (and therefore the topological transition) occurs at the threshold energy, where minima first outnumber saddle points.

Given the controversy surrounding the threshold energy described in the introduction, it may be surprising that we find it is the level at which the microcanonical configuration space becomes typically disconnected. However, very recent work suggests that prior conclusions questioning its dynamic significance may have been based on transient behavior, at least for the models we describe here [62,63]. But  $E_{\text{th}}$  cannot hold its dynamic significance in *all* models, because in some cases it can fall beneath the energy  $E_{\text{alg}}$  proven to bound the performance of polynomial-time algorithms, including all physical dynamics [64,65].

Since  $E_{\text{alg}}$  also is the lowest energy at which *any* connected component of the level set exists (see Fig. 2), the topological transition studied here must also differ from  $E_{\text{th}}$  for these models [54]. The importance of  $E_{\text{alg}}$  results from the difficulty of dynamics to navigate the landscape in the absence of a large connected component; given the elementary greedy nature of gradient descent, we suspect it stalls when a large connected component becomes atypical even when this does not correspond to  $E_{\text{th}}$ . Understanding the nature of the energy landscape and its relationship to out-of-equilibrium dynamics in such models is a priority for future research. We do not expect the threshold energy usually holds this topological significance in more structured mean-field models and in finite-dimensional systems.

The conjectured connection between infinite persistence and topological transitions in configuration space should be studied in systems outside of mean field. Already, existing work on the random Lorentz gas is consistent with this conjecture, though it is also a toy model [36]. Making a similar analysis of hard or soft spheres may be restricted by the current understanding of the topological properties of their configuration space; detailed analysis currently exists only for systems of relatively few particles, for which all walks are ergodic [66–69]. In the absence of direct topological approaches, this method may advance our understanding of the topology of configurations in particle systems. Numeric techniques developed for simulating infinitely persistent activity [39] may permit the same analysis in finite-dimensional systems, like active hard- and soft-sphere glasses [40]. Mean-field liquids may admit an analytic approach, extending the existing dynamical mean-field theory for infinitely persistent active fluids [38] by adding a microcanonical energy constraint.

*Acknowledgments*—The authors thank James P Sethna, Ralph B Robinson, and Bethany Dixon at Cornell University for providing and facilitating access to computing resources used in this work, and thank Johannes Lang for useful conversations. J. K.-D. is supported by FAPESP Young Investigator Grant No. 2024/11114-1. J. K.-D. also received support from the Simons Foundation Targeted Grant to ICTP-SAIFR.

*Data availability*—The data that support the findings of this article are openly available [70,71].

- 
- [1] F. H. Stillinger and T. A. Weber, Packing structures and transitions in liquids and solids, *Science* **225**, 983 (1984).
  - [2] T. Castellani and A. Cavagna, Spin-glass theory for pedestrians, *J. Stat. Mech.* (2005) P05012.
  - [3] J. N. Onuchic, Z. Luthey-Schulten, and P. G. Wolynes, Theory of protein folding: The energy landscape perspective, *Annu. Rev. Phys. Chem.* **48**, 545 (1997).

- [4] S. J. Arnold, M. E. Pfrender, and A. G. Jones, The adaptive landscape as a conceptual bridge between micro- and macroevolution, *Genetica* **112/113**, 9 (2001).
- [5] A. Altieri, F. Roy, C. Cammarota, and G. Biroli, Properties of equilibria and glassy phases of the random Lotka-Volterra model with demographic noise, *Phys. Rev. Lett.* **126**, 258301 (2021).
- [6] A. J. Ballard, R. Das, S. Martiniani, D. Mehta, L. Sagun, J. D. Stevenson, and D. J. Wales, Energy landscapes for machine learning, *Phys. Chem. Chem. Phys.* **19**, 12585 (2017).
- [7] F. Draxler, K. Veschgini, M. Salmhofer, and F. Hamprecht, Essentially no barriers in neural network energy landscape, in *Proceedings of the 35th International Conference on Machine Learning*, Proceedings of Machine Learning Research Vol. 80, edited by J. Dy and A. Krause (PMLR, Stockholm, Sweden, 2018), pp. 1309–1318.
- [8] J. B. Tenenbaum, A global geometric framework for nonlinear dimensionality reduction, *Science* **290**, 2319 (2000).
- [9] L. van der Maaten and G. Hinton, Visualizing data using t-SNE, *J. Mach. Learn. Res.* **9**, 2579 (2008), <http://jmlr.org/papers/v9/vandermaaten08a.html>.
- [10] K. R. Moon, D. van Dijk, Z. Wang, S. Gigante, D. B. Burkhardt, W. S. Chen, K. Yim, A. van den Elzen, M. J. Hirn, R. R. Coifman, N. B. Ivanova, G. Wolf, and S. Krishnaswamy, Visualizing structure and transitions in high-dimensional biological data, *Nat. Biotechnol.* **37**, 1482 (2019).
- [11] H. K. Teoh, K. N. Quinn, J. Kent-Dobias, C. B. Clement, Q. Xu, and J. P. Sethna, Visualizing probabilistic models in Minkowski space with intensive symmetrized Kullback-Leibler embedding, *Phys. Rev. Res.* **2**, 033221 (2020).
- [12] A. J. Bray and M. A. Moore, Metastable states in spin glasses, *J. Phys. C* **13**, L469 (1980).
- [13] H. Rieger, The number of solutions of the Thouless-Anderson-Palmer equations for  $p$ -spin-interaction spin glasses, *Phys. Rev. B* **46**, 14655 (1992).
- [14] A. Cavagna, I. Giardina, and G. Parisi, An investigation of the hidden structure of states in a mean-field spin-glass model, *J. Phys. A* **30**, 7021 (1997).
- [15] V. Ros and Y. V. Fyodorov, The high-dimensional landscape paradigm: Spin-glasses, and beyond, in *Spin Glass Theory and Far Beyond* (World Scientific, Singapore, 2023), pp. 95–114.
- [16] J. Kurchan and L. Laloux, Phase space geometry and slow dynamics, *J. Phys. A* **29**, 1929 (1996).
- [17] L. F. Cugliandolo and J. Kurchan, Analytical solution of the off-equilibrium dynamics of a long-range spin-glass model, *Phys. Rev. Lett.* **71**, 173 (1993).
- [18] G. Ben Arous, E. Subag, and O. Zeitouni, Geometry and temperature chaos in mixed spherical spin glasses at low temperature: The perturbative regime, *Commun. Pure Appl. Math.* **73**, 1732 (2019).
- [19] G. Folena, S. Franz, and F. Ricci-Tersenghi, Rethinking mean-field glassy dynamics and its relation with the energy landscape: The surprising case of the spherical mixed  $p$ -spin model, *Phys. Rev. X* **10**, 031045 (2020).
- [20] J. Kent-Dobias and J. Kurchan, How to count in hierarchical landscapes: A full solution to mean-field complexity, *Phys. Rev. E* **107**, 064111 (2023).
- [21] J. Kent-Dobias, Conditioning the complexity of random landscapes on marginal optima, *Phys. Rev. E* **110**, 064148 (2024).
- [22] J. Kent-Dobias, Algorithm-independent bounds on complex optimization through the statistics of marginal optima, [arXiv:2407.02092](https://arxiv.org/abs/2407.02092).
- [23] G. Folena, S. Franz, and F. Ricci-Tersenghi, Gradient descent dynamics in the mixed  $p$ -spin spherical model: Finite-size simulations and comparison with mean-field integration, *J. Stat. Mech.* (2021) P033302.
- [24] G. Folena and F. Zamponi, On weak ergodicity breaking in mean-field spin glasses, *SciPost Phys.* **15**, 109 (2023).
- [25] J. Kent-Dobias, On the topology of solutions to random continuous constraint satisfaction problems, *SciPost Phys.* **18**, 158 (2025).
- [26] S. Ramaswamy, Active matter, *J. Stat. Mech.* (2017) P054002.
- [27] L. Caprini, U. Marini Bettolo Marconi, A. Puglisi, and A. Vulpiani, Active escape dynamics: The effect of persistence on barrier crossing, *J. Chem. Phys.* **150**, 024902 (2019).
- [28] E. Woillez, Y. Zhao, Y. Kafri, V. Lecomte, and J. Tailleur, Activated escape of a self-propelled particle from a metastable state, *Phys. Rev. Lett.* **122**, 258001 (2019).
- [29] L. Zanollo, M. Caraglio, T. Franosch, and P. Faccioli, Target search of active agents crossing high energy barriers, *Phys. Rev. Lett.* **126**, 018001 (2021).
- [30] F. Coghi, R. Duvezin, and J. S. Wettlaufer, Accelerated first-passage dynamics in a non-Markovian feedback Ornstein-Uhlenbeck process, *J. Stat. Phys.* **192**, 128 (2025).
- [31] L. Berthier and J. Kurchan, Non-equilibrium glass transitions in driven and active matter, *Nat. Phys.* **9**, 310 (2013).
- [32] S. K. Nandi, R. Mandal, P. J. Bhuyan, C. Dasgupta, M. Rao, and N. S. Gov, A random first-order transition theory for an active glass, *Proc. Natl. Acad. Sci. U.S.A.* **115**, 7688 (2018).
- [33] G. Biroli, P. Charbonneau, E. I. Corwin, Y. Hu, H. Ikeda, G. Szamel, and F. Zamponi, Interplay between percolation and glassiness in the random Lorentz gas, *Phys. Rev. E* **103**, L030104 (2021).
- [34] G. Biroli, P. Charbonneau, Y. Hu, H. Ikeda, G. Szamel, and F. Zamponi, Mean-field caging in a random Lorentz gas, *J. Phys. Chem. B* **125**, 6244 (2021).
- [35] B. Charbonneau, P. Charbonneau, Y. Hu, and Z. Yang, High-dimensional percolation criticality and hints of mean-field-like caging of the random Lorentz gas, *Phys. Rev. E* **104**, 024137 (2021).
- [36] M. Zheng, D. Khomenko, and P. Charbonneau, Not-so-glass-like caging and fluctuations of an active matter model, *Phys. Rev. Lett.* **134**, 228301 (2025).
- [37] P. K. Morse, S. Roy, E. Agoritsas, E. Stanifer, E. I. Corwin, and M. L. Manning, A direct link between active matter and sheared granular systems, *Proc. Natl. Acad. Sci. U.S.A.* **118**, e2019909118 (2021).
- [38] E. Agoritsas, Mean-field dynamics of infinite-dimensional particle systems: Global shear versus random local forcing, *J. Stat. Mech.* (2021) P033501.
- [39] R. Mandal and P. Sollich, How to study a persistent active glassy system, *J. Phys. Condens. Matter* **33**, 184001 (2021).

- [40] Y.-E. Keta, R. Mandal, P. Sollich, R. L. Jack, and L. Berthier, Intermittent relaxation and avalanches in extremely persistent active matter, *Soft Matter* **19**, 3871 (2023).
- [41] D. Martin, J. O’Byrne, M. E. Cates, E. Fodor, C. Nardini, J. Tailleur, and F. van Wijland, Statistical mechanics of active Ornstein-Uhlenbeck particles, *Phys. Rev. E* **103**, 032607 (2021).
- [42] T. R. Kirkpatrick and D. Thirumalai,  $p$ -spin-interaction spin-glass models: Connections with the structural glass problem, *Phys. Rev. B* **36**, 5388 (1987).
- [43] T. R. Kirkpatrick and P. G. Wolynes, Connections between some kinetic and equilibrium theories of the glass transition, *Phys. Rev. A* **35**, 3072 (1987).
- [44] T. R. Kirkpatrick and P. G. Wolynes, Stable and metastable states in mean-field Potts and structural glasses, *Phys. Rev. B* **36**, 8552 (1987).
- [45] T. R. Kirkpatrick and D. Thirumalai, Colloquium: Random first order transition theory concepts in biology and physics, *Rev. Mod. Phys.* **87**, 183 (2015).
- [46] A. Crisanti and H.-J. Sommers, The spherical  $p$ -spin interaction spin glass model: The statics, *Z. Phys. B Condens. Matter* **87**, 341 (1992).
- [47] A. Crisanti, H. Horner, and H.-J. Sommers, The spherical  $p$ -spin interaction spin-glass model: The dynamics, *Z. Phys. B Condens. Matter* **92**, 257 (1993).
- [48] A. Crisanti and H.-J. Sommers, Thouless-Anderson-Palmer approach to the spherical  $p$ -spin spin glass model, *J. Phys. I (France)* **5**, 805 (1995).
- [49] A. Cavagna, I. Giardina, and G. Parisi, Stationary points of the Thouless-Anderson-Palmer free energy, *Phys. Rev. B* **57**, 11251 (1998).
- [50] A. Crisanti and L. Leuzzi, Spherical  $2 + p$  spin-glass model: An analytically solvable model with a glass-to-glass transition, *Phys. Rev. B* **73**, 014412 (2006).
- [51] A. Auffinger, G. Ben Arous, and J. Černý, Random matrices and complexity of spin glasses, *Commun. Pure Appl. Math.* **66**, 165 (2012).
- [52] A. Auffinger and G. Ben Arous, Complexity of random smooth functions on the high-dimensional sphere, *Ann. Probab.* **41**, 4214 (2013).
- [53] J. Kent-Dobias, When is the average number of saddle points typical?, *Europhys. Lett.* **143**, 61003 (2023).
- [54] D. Gamarnik, The overlap gap property: A topological barrier to optimizing over random structures, *Proc. Natl. Acad. Sci. U.S.A.* **118**, e2108492118 (2021).
- [55] L. F. Cugliandolo, Dynamics of glassy systems, [arXiv:cond-mat/0210312](https://arxiv.org/abs/cond-mat/0210312).
- [56] L. Caprini, A. Puglisi, and A. Sarracino, Fluctuation–dissipation relations in active matter systems, *Symmetry* **13**, 81 (2021).
- [57] L. F. Cugliandolo, J. Kurchan, P. Le Doussal, and L. Peliti, Glassy behaviour in disordered systems with nonrelaxational dynamics, *Phys. Rev. Lett.* **78**, 350 (1997).
- [58] L. Berthier, J.-L. Barrat, and J. Kurchan, A two-time-scale, two-temperature scenario for nonlinear rheology, *Phys. Rev. E* **61**, 5464 (2000).
- [59] E. Leutheusser, Dynamical model of the liquid-glass transition, *Phys. Rev. A* **29**, 2765 (1984).
- [60] U. Bengtzelius, W. Gotze, and A. Sjolander, Dynamics of supercooled liquids and the glass transition, *J. Phys. C* **17**, 5915 (1984).
- [61] F. Caltagirone, U. Ferrari, L. Leuzzi, G. Parisi, F. Ricci-Tersenghi, and T. Rizzo, Critical slowing down exponents of mode coupling theory, *Phys. Rev. Lett.* **108**, 085702 (2012).
- [62] J. Lang, S. Sachdev, and S. Diehl, Numerical renormalization of glassy dynamics, *Phys. Rev. Lett.* **135**, 247101 (2025).
- [63] J. Lang (private communication).
- [64] A. El Alaoui and A. Montanari, Algorithmic thresholds in mean field spin glasses, [arXiv:2009.11481v1](https://arxiv.org/abs/2009.11481v1).
- [65] A. El Alaoui, A. Montanari, and M. Sellke, Optimization of mean-field spin glasses, *Ann. Probab.* **49**, 2922 (2021).
- [66] G. Carlsson, J. Gorham, M. Kahle, and J. Mason, Computational topology for configuration spaces of hard disks, *Phys. Rev. E* **85**, 011303 (2012).
- [67] M. Barnett-Jones, P. A. Dickinson, M. J. Godfrey, T. Grundy, and M. A. Moore, Transition state theory and the dynamics of hard disks, *Phys. Rev. E* **88**, 052132 (2013).
- [68] E. R. Weeks and K. Criddle, Visualizing free-energy landscapes for four hard disks, *Phys. Rev. E* **102**, 062153 (2020).
- [69] O. B. Eriçok, K. Ganesan, and J. K. Mason, Configuration spaces of hard spheres, *Phys. Rev. E* **104**, 055304 (2021).
- [70] J. Kent-Dobias, Log-Fourier integrator (2025), [https://github.com/kentdobias/level-set\\_walks](https://github.com/kentdobias/level-set_walks).
- [71] J. Kent-Dobias, Data necessary to reproduce results of “very persistent random walkers reveal transitions in landscape topology”, [10.5281/zenodo.18682166](https://zenodo.org/record/18682166) (2026).
- [72] J. Kurchan, Supersymmetry in spin glass dynamics, *J. Phys. I (France)* **2**, 1333 (1992).
- [73] G. V. Haines and A. G. Jones, Logarithmic Fourier transformation, *Geophys. J. Int.* **92**, 171 (1988).
- [74] J. Lang and B. Frank, Fast logarithmic Fourier-Laplace transform of nonintegrable functions, *Phys. Rev. E* **100**, 053302 (2019).
- [75] L. F. Cugliandolo (private communication).
- [76] M. Frigo and S. Johnson, The design and implementation of FFTW3, *Proc. IEEE* **93**, 216 (2005).

## End Matter

*Deriving the dynamical equations*—The procedure for writing the dynamical equations above is not novel [55], but it is worth following aspects of it carefully to see how the generalized fluctuation-dissipation relation arises. Solutions to the Langevin equation (3) can be sampled using the path integral

$$Z = \int \mathcal{D}\mathbf{x} \mathcal{D}\mu \mathcal{D}\beta \delta(\xi_t - \partial_t \mathbf{x}_t - \mu_t \mathbf{x}_t - \beta_t \nabla H(\mathbf{x}_t)) \times \delta\left(\frac{1}{2}(N - \|\mathbf{x}_t\|^2)\right) \delta(NE - H(\mathbf{x}_t)) \times \det \begin{bmatrix} [I(\partial_t + \mu_t) + \beta_t \nabla^2 H(\mathbf{x}_t)] \delta_{ts} & \mathbf{x}_t \delta_{ts} & \nabla H(\mathbf{x}_t) \delta_{ts} \\ \mathbf{x}_s \delta_{ts} & 0 & 0 \\ \nabla H(\mathbf{x}_s) \delta_{ts} & 0 & 0 \end{bmatrix}. \quad (\text{A1})$$

The integrand is converted to an exponential function by writing the  $\delta$  functions in their Fourier representations and by writing the determinant with Grassmann variables. In this form the noise can be averaged away. The result is compactly represented with superspace coordinates: introducing Grassmann indices  $\bar{\theta}$  and  $\theta$  and defining  $a = (t, \theta, \bar{\theta})$ , we write

$$\phi_a = \mathbf{x}_t + \bar{\theta} \bar{\eta}_t + \bar{\eta}_t \theta + \bar{\theta} \hat{x}_t, \quad (\text{A2})$$

$$B_a = \beta_t + \bar{\theta} \bar{\gamma}_t + \bar{\gamma}_t \theta + \bar{\theta} \hat{\beta}_t, \quad (\text{A3})$$

$$\Lambda_a = \mu_t + \bar{\theta} \bar{\vartheta}_t + \bar{\vartheta}_t \theta + \bar{\theta} \hat{\mu}_t, \quad (\text{A4})$$

for Grassmann fields  $\bar{\eta}$ ,  $\eta$ ,  $\bar{\gamma}$ ,  $\gamma$ ,  $\bar{\vartheta}$ , and  $\vartheta$ , and auxiliary real-valued fields  $\hat{x}$ ,  $\hat{\beta}$ , and  $\hat{\mu}$ . The result is

$$\langle Z \rangle = \int \mathcal{D}\phi \mathcal{D}B \mathcal{D}\Lambda \exp \left\{ \int da \left[ \frac{1}{2} \phi_a^T D_a^{(2)} \phi_a + \frac{1}{2} \Lambda_a (N - \|\phi_a\|^2) + B_a (NE - H(\phi_a)) \right] \right\}. \quad (\text{A5})$$

The differential operator that produces the kinetic part of the action is defined by

$$D_a^{(2)} \psi = 2\Gamma * \frac{\partial^2 \psi}{\partial \bar{\theta} \partial \theta} + 2\theta \frac{\partial^2 \psi}{\partial \theta \partial t} - \frac{\partial \psi}{\partial t}, \quad (\text{A6})$$

where  $*$  denotes convolution in the time coordinate. Averaging over the disorder in  $H$  and introducing order parameters  $Q_{ab} = (1/N) \phi_a \cdot \phi_b$ , we find an effective action

$$\mathcal{S}(Q, B, \Lambda) = \int da \left[ \frac{1}{2} \Lambda_a + B_a E \right] + \frac{1}{2} \log \det Q + \frac{1}{2} \int da db \left[ \delta_{ab} (D_a^{(2)} - \Lambda_a) Q_{ab} + B_a B_b f(Q_{ab}) \right]. \quad (\text{A7})$$

Differentiating with respect to the order parameters to extremize the action results in the equations

$$0 = (D_a^{(2)} - \Lambda_a) Q_{ab} + \int dc B_a B_c f'(Q_{ac}) Q_{cb} + I_{ab}, \quad (\text{A8})$$

$$0 = \int db B_b f(Q_{ab}) + E, \quad 0 = Q_{aa} - 1. \quad (\text{A9})$$

The action of the path integral (A5) is invariant under the action of the set of operators [72]

$$\bar{D}'_a \psi = \Gamma * \frac{\partial \psi}{\partial \theta} + \bar{\theta} \frac{\partial \psi}{\partial t}, \quad D_a \psi = \Gamma * \frac{\partial \psi}{\partial \bar{\theta}} - \theta \frac{\partial \psi}{\partial t}, \quad (\text{A10})$$

$$D'_a \psi = \frac{\partial \psi}{\partial \bar{\theta}}, \quad \bar{D}_a \psi = \frac{\partial \psi}{\partial \theta}, \quad (\text{A11})$$

$$[\bar{D}'_a, D'_a]_+ \psi = \frac{\partial \psi}{\partial t}, \quad [\bar{D}_a, D_a]_+ \psi = -\frac{\partial \psi}{\partial t}. \quad (\text{A12})$$

In particular the kinetic term  $D_a^{(2)} = [\bar{D}_a, D_a]_-$ . The symmetry with respect to these operators and their two-component generalizations  $\mathbf{D}'_{ab} = D'_a + D'_b$ ,  $\bar{\mathbf{D}}'_{ab} = \bar{D}'_a + \bar{D}'_b$ , and  $[\bar{\mathbf{D}}'_{ab}, \mathbf{D}'_{ab}]_+ = (\partial/\partial t) + (\partial/\partial s)$  imply Ward identities constraining the order parameters. The resulting Ward identities imply the vanishing of all fermionic order parameters,  $\hat{\mu}$  and  $\hat{\beta}$ , and the order parameter corresponding to  $\hat{x} \cdot \hat{x}$ . They also imply time-translation invariance, and the fluctuation-dissipation relation (11) is implied by the Ward identity associated with  $\bar{\mathbf{D}}'$ . Expanding the superspace notation of (A8) and (A9) and applying these Ward identities results in (8)–(10), with  $C(\tau) = (1/N) \mathbf{x}_{t+\tau} \cdot \mathbf{x}_t$  and  $R(\tau) = (1/N) \mathbf{x}_{t+\tau} \cdot \hat{\mathbf{x}}_t$ .

*Exact solution for the 2-spin model*—For the 2-spin model, with  $f(q) = \frac{1}{2} q^2$ , the dynamical equations are exactly solvable. Written in Fourier space, they are

$$(i\omega + \mu) \hat{C}(\omega) = 2\hat{\Gamma}(\omega) \hat{R}(\omega)^\dagger + \beta^2 \hat{C}(\omega) [\hat{R}(\omega) + \hat{R}(\omega)^\dagger], \quad (i\omega + \mu) \hat{R}(\omega) = 1 + \beta^2 \hat{R}(\omega)^2. \quad (\text{B1})$$

This is quadratic in  $\hat{C}$  and  $\hat{R}$  and can be directly solved. The general solution is not helpful to share here, but the

ergodicity-breaking transition occurs when  $\beta = \frac{1}{2}\mu$ , where  $\hat{C}$  develops a cusp singularity at  $\omega = 0$  and takes the form

$$\hat{C}(\omega) = \frac{1}{\mu^3 \omega^2 (1 + \tau_0^2 \omega^2)} \left[ \left( \omega^2 + |\omega| \sqrt{4\mu^2 + \omega^2} \right) \times \sqrt{2|\omega| \sqrt{4\mu^2 + \omega^2} - 2\omega^2 - 4\mu\omega^2} \right]. \quad (\text{B2})$$

The spherical constraint requires

$$1 = C(0) = \frac{1}{2\pi} \int d\omega \hat{C}(\omega) = 2 \frac{\sqrt{1 + 2\tau_0\mu} - 1}{\tau_0\mu^2}, \quad (\text{B3})$$

which implies that

$$\mu = 4 \sqrt{\frac{1}{3\tau_0} \sinh \left[ \frac{1}{3} \sinh^{-1} \left( \frac{3}{2} \sqrt{3\tau_0} \right) \right]}. \quad (\text{B4})$$

The energy of the transition is then

$$E_d = -\frac{\mu}{2} \int d\tau C(\tau) R(\tau) = -\frac{\mu}{4\pi} \int d\omega \hat{C}(\omega) \hat{R}(\omega), \quad (\text{B5})$$

which when evaluated produces the formula in the text. We can also work directly at  $\tau_0 = \infty$ . Scaling  $\omega$  with  $\tau_0$ , we find

$$\lim_{\tau_0 \rightarrow \infty} \hat{C}(\nu/\tau_0) = \frac{1}{\beta^2} \frac{\mu \left[ \mu - \sqrt{\mu^2 - 4\beta^2} \right] - 4\beta^2}{(4\beta^2 - \mu^2)(1 + \nu^2)}. \quad (\text{B6})$$

This is the Fourier form for a simple exponential.  $C(0) = 1$  gives

$$\mu = \frac{1 + 2\beta^2}{\sqrt{1 + \beta^2}}, \quad (\text{B7})$$

and then for the energy we have

$$\lim_{\tau_0 \rightarrow \infty} \hat{C}(\nu/\tau_0) \hat{R}(\nu/\tau_0) = \frac{2}{\sqrt{1 + \beta^2}} \frac{1}{1 + \nu^2}, \quad (\text{B8})$$

yielding  $E = -(1 + \beta^{-2})^{-\frac{1}{2}}$ . The dynamic transition occurs at  $\beta = \infty$ . This gives the scaling  $E = -1 + \frac{1}{2}\beta^{-2} + O(\beta^{-4})$  cited in the main text.

*Iteration scheme for numeric solutions*—To find numeric solutions to the dynamical equations, we use an iterative scheme. We start from the exact solutions for  $C$  and  $R$  at  $E = \beta = 0$ ,

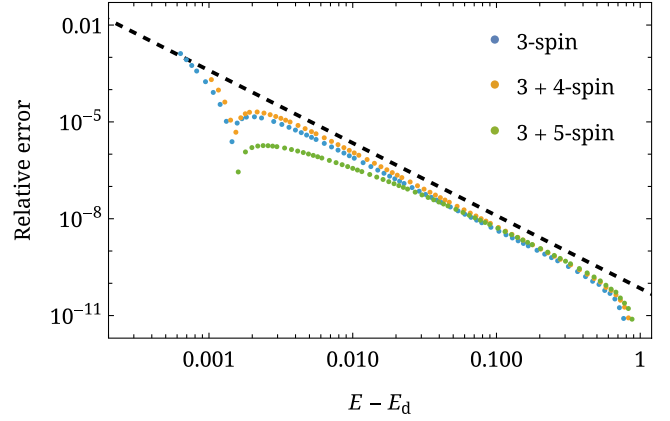


FIG. 6. Estimation of error in the numeric method using results for  $\tau_0 = 0$ , where the equilibrium dynamics imply  $E = -f(1)\beta$  and the error  $|\tilde{E} - E|/|E_d - E|$  relative to the distance from the dynamic transition  $E_d$  can be measured. The relative error grows as  $E_d$  is approached. The dashed black line shows  $(E - E_d)^{-2.25}$  and is meant as a guide. The smallest differences  $E - E_{th}$  used in this Letter are around  $2 \times 10^{-4}$ , where the extrapolated error is around 2%.

$$C_0(\tau) = \frac{\mu_0^{-1} e^{-\mu_0\tau} - \tau_0 e^{-\tau/\tau_0}}{1 - \mu_0^2 \tau_0^2}, \quad R_0(\tau) = \Theta(\tau) e^{-\mu_0\tau}, \quad (\text{C1})$$

where

$$\mu_0 = \frac{\sqrt{1 + 4\tau_0} - 1}{2\tau_0}. \quad (\text{C2})$$

To speed convergence,  $\beta$  is fixed and a numeric estimate  $\tilde{E}$  for the energy determined after convergence. At each step, the self-energies are computed using the current estimates of  $C$  and  $R$  using

$$\Sigma_n(\tau) = \beta^2 R_n(\tau) f''(C_n(\tau)) \quad D_n(\tau) = \beta^2 f'(C_n(\tau)). \quad (\text{C3})$$

Fourier transforming these functions, we then set  $C$  and  $R$  for the next iteration through their Fourier transforms

$$\hat{C}_{n+1}(\omega) = \frac{[2\hat{\Gamma}(\omega) + \hat{D}_n(\omega)]\hat{R}_n(\omega)^\dagger + \hat{\Sigma}_n(\omega)\hat{C}_n(\omega)}{i\omega + \mu_{n+1}}, \quad (\text{C4})$$

$$\hat{R}_{n+1}(\omega) = \frac{1 + \hat{\Sigma}_n(\omega)\hat{R}_n(\omega)}{i\omega + \mu_{n+1}},$$

where  $\mu_{n+1}$  is set by the requirement that  $C_{n+1}(0) = 1$  and is determined by binary search. The iteration is continued until the integrated root mean square of the dynamical equations is less than some threshold. We discretize the Fourier transform using logarithmic spacing of  $\omega$ , which strongly benefits the precision of the result [73,74]. The method appears to be fundamentally unstable for models containing any 2-spin

component, something long known for iterative methods [75].

For the data presented here, we represented the correlation and response functions using 80-bit floating point numbers on an evenly log-spaced grid of  $2^{15}$  points spanning the interval  $(5.9 \times 10^{-15}, 1.7 \times 10^{14})/\mu_0$ . The Fourier transforms were made on a domain of  $4 \times 2^{15}$  points, padded with the time-reflected function and zeroes.

After every step,  $C$  and  $R$  were cropped in the range  $[0, 1]$  and monotony enforced. The iteration was considered converged when the rms average over the frequency grid of the difference between the right- and left-hand sides of Eqs. (8) and (9) fell below  $10^{-13}$ . Fourier transforms were carried out using the FFTW library [76]. The code used is publicly available [70]. An estimate of the error due to the method with these parameters is shown in Fig. 6.